Experimental demonstration of the physics of resonant cavities

J. Pellicer-Porres[a] and M. V. Andrés
ICMUV, Universidad de Valencia, c/Dr. Moliner 50, 46100 Burjassot, Valencia, Spain

(Received 11 May 2004; accepted 26 October 2004)

We describe an undergraduate experiment that demonstrates the physics of cavity resonators. A mobile wall lets students alter the position of the nodes, thus changing the mode pattern. The nodal structure is made apparent by placing a metallic plate at different positions inside the cavity. A technique for dielectric characterization also is introduced, which helps students understand the boundary conditions in dielectrics, as well as highlighting the characteristics of fields in cavities.
[DOI: 10.1119/1.1834921]

I. INTRODUCTION

Resonant cavities are analogous to an LC oscillator in the microwave spectral region, and often are part of microwave circuits. The introduction of a dielectric in a resonator is the best way to measure the dielectric constant at microwave frequencies. We describe a laboratory experiment based on a cavity resonator. The use of a cavity resonator in an undergraduate laboratory demonstrates the concept of resonance. The cavity is easy to construct and can be designed to allow for modifications of its resonant conditions by the movement of one of the walls. Different modes can be selected by setting a metallic plate at given positions within the cavity.

We also introduce the dielectric characterization procedure used with the cavity. The theory is based on a perturbation method and shows alternative ways of extracting information when a direct approach is not possible. The solution demonstrates the behavior of the field and is a good example of the application of boundary conditions. We choose a rectangular geometry so that the theory does not involve functions that may obscure the physics.

II. EXPERIMENTAL SETUP

The resonator consists of a rectangular aluminum cavity with dimensions $a=98$ cm, $b=49.8$ cm, and $d=25$ cm (see Fig. 1). The smallest wall is mobile, so the length a of the cavity may be varied. This wall also may be removed to gain access to the cavity.

Electromagnetic fields are established and detected in the cavity by means of loops attached to the smallest walls. The loops are positioned perpendicular to the walls to maximize the magnetic flux. Loops are impedance-matched to coaxial lines by introducing 50 Ω resistors in series.

Our system includes a Hameg HM8028 spectrum analyzer coupled to a HM8038 tracking generator and to an oscilloscope. The tracking generator yields a constant amplitude harmonic signal, whose frequency may be varied between 0 Hz and 500 MHz. The spectrum analyzer measures the signal amplitude at each frequency, and the oscilloscope displays the detected amplitude versus the frequency.

III. DISCUSSION

A. Basic cavity characterization

Electromagnetic fields inside the cavity obey the wave equation.[1–4] In a rectangular geometry the wave equation can be solved by separation of variables, and its solution can be expressed in terms of plane waves. The complete determination of the electromagnetic fields requires the introduction of boundary conditions. If we consider the metallic cavity walls as perfect conductors, the electric field must be perpendicular to the walls, and the magnetic field must be tangential to the metallic surfaces. This set of boundary conditions is highly restrictive, and determines the appearance of standing waves with certain characteristic oscillation frequencies. The electric field can be written as:[1,2]

$$E_x = E_x^0 \cos(k_x x)\,\sin(k_y y)\sin(k_z z)e^{-i\omega t}, \tag{1a}$$

$$E_y = E_y^0 \sin(k_x x)\cos(k_y y)\sin(k_z z)e^{-i\omega t}, \tag{1b}$$

$$E_z = E_z^0 \sin(k_x x)\sin(k_y y)\cos(k_z z)e^{-i\omega t}. \tag{1c}$$

Note that the E_x component is finite in the yz plane ($x=0$), but the E_y and E_z components vanish. The same condition is required at the opposite wall ($x=a$), so $k_x = m\pi/a$, or equivalently, $\lambda = 2a/m$, where m is an integer. Similarly $k_y = n\pi/b$ and $k_z = p\pi/d$, with

$$k^2 = \frac{\omega^2}{c^2} = \left(m\frac{\pi}{a}\right)^2 + \left(n\frac{\pi}{b}\right)^2 + \left(p\frac{\pi}{d}\right)^2. \tag{2}$$

It can be shown that $\vec{H} = (\vec{k}\times\vec{E})/i\mu_0\omega$ also satisfies the boundary conditions. The full derivation of Eq. (1) and other technical details can be found in Ref. 1.

We observe the frequencies $f_{110} = 340 \pm 1$ MHz and $f_{210} = 434 \pm 2$ MHz in the resonator. Figure 2(a) shows the trace observed on the oscilloscope, which corresponds to the transmission of the cavity in the frequency range [150, 500] MHz. The first question is why these particular modes arise and how their important characteristics can be shown to students.

From Eq. (1) we see that at least two of the integers m, n, and p must be different from zero to have nonvanishing fields. The lowest frequency, f_{110}, has nonzero integers associated with the larger cavity dimensions, and thus the nodes are as separated as possible. The next frequency, f_{210}, doubles the periodicity in the largest direction, and the frequency is increased by the smallest step. Other modes are out of our system's bandwidth.

The smallest side of the cavity in our resonator is mobile, and the position of the nodes can be easily altered. Decreasing the distance between the nodes will increase the resonance frequency. In Fig. 3 we represent f_{110}^2 and f_{210}^2 as a function of $1/a^2$. A linear fit to the curves yields a determination of the velocity of light in vacuum using Eq. (2). We

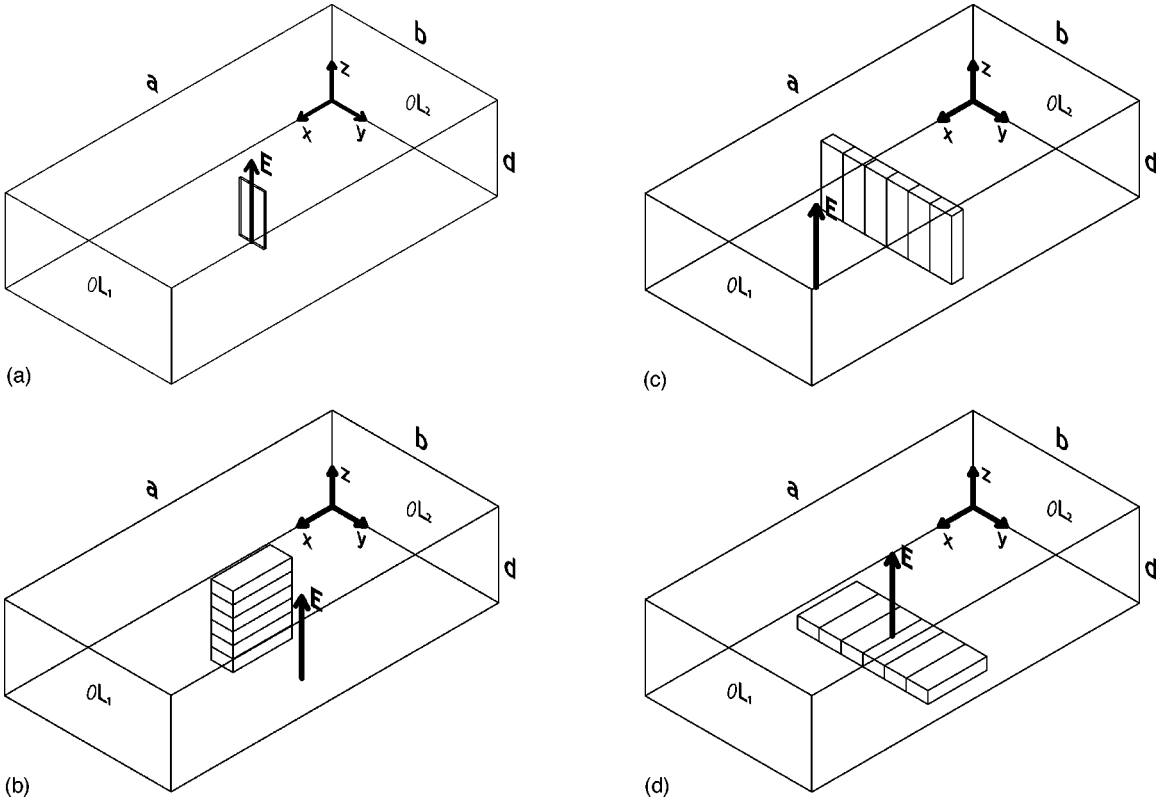

Fig. 1. The rectangular cavity used in the demonstration. L_1 and L_2 represent the loops that we used to generate the fields and to measure the transmission through the cavity. In (a) we have represented the metallic plate used to suppress the (110) mode. In (b) several dielectric blocks are piled along the z axis. In (c) and (d) the blocks are piled horizontally, side by side, maintaining the symmetric position of the blocks around the cavity center. The blocks in (d) are rotated 90° with respect to configuration (c). In (b) and (c) $E^0_{\text{int}} \approx E^0_z$; in (d) $\epsilon E^0_{\text{int}} \approx \epsilon_0 E^0_z$.

obtained $c=(2.97\pm0.03)\times10^8$ m/s and $c=(2.95\pm0.07)\times10^8$ m/s from the data corresponding to the (110) and (210) modes, respectively.

In the two observed modes $p=0$. Thus, according to Eq. (1), the electric field has only one component, E_z. In the f_{110} mode E increases along the x or y directions up to the center of the cavity, where it has an absolute maximum, and then decreases to zero at the cavity walls. The electric field is uniform along the z direction. The field distribution corresponding to the f_{210} mode is similar, except for its dependence on the x coordinate, where the double periodicity introduces a node in the center of the cavity.

The electric field characteristics of both modes can be readily explored in our apparatus. When a metallic plate ($7.5\times20.3\times0.2$ cm^3) is situated at the center of the cavity as indicated in Fig. 1(a), the (110) mode is suppressed. However, the (210) mode, whose electric field is zero at the center

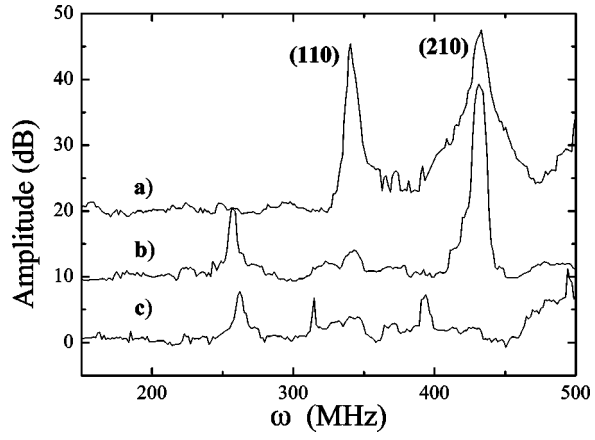

Fig. 2. Experimental transmittance as observed on the oscilloscope. (a) In the empty cavity the (110) and (210) modes are apparent. (b) The introduction of a metallic plate in the center of the cavity suppresses the (110) mode. (c) If the metallic plate is displaced, both modes disappear. Curves (a) and (b) have been shifted for clarity.

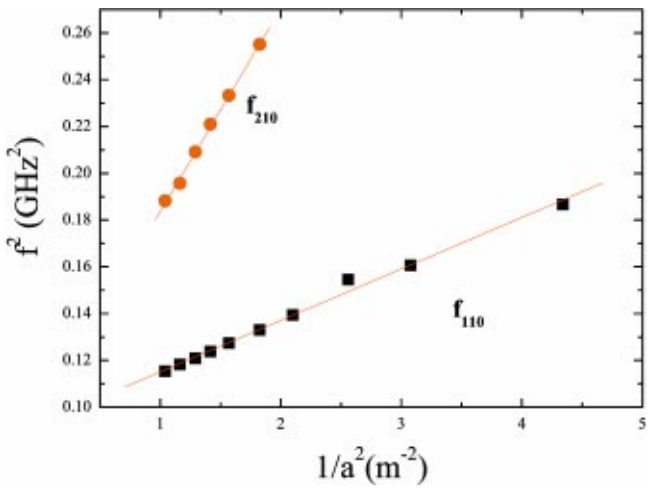

Fig. 3. The dependence of the resonant frequency on the cavity dimensions. The slopes are related to the velocity of light.

of the cavity, is still observed. To suppress both the (110) and the (210) modes, it is necessary to shift the metallic plate to a position where the fields associated with both modes are finite. Figure 2 summarizes these phenomena. The spurious peaks that appear when the metallic plate is introduced are at least 80 times weaker (19 dB) than the (210) mode.

B. Cavity with a dielectric

The introduction of a dielectric in the resonator shifts the frequencies associated with standing waves. To investigate the modifications, we use a perturbation method with the original resonator as a reference. The change in frequency is given by[4]

$$\frac{\omega-\omega_0}{\omega}=\frac{-\int_{V_d}\Delta\epsilon\vec{E}\cdot\vec{E}_0^*\,dV}{\int_{V_c}(\epsilon\vec{E}\cdot\vec{E}_0^*+\mu_0\vec{H}\cdot\vec{H}_0^*)\;\;dV}. \tag{3}$$

The subscript 0 refers to the unperturbed system, and V_d and V_c are the dielectric and cavity volumes, respectively. Equation (3) is exact provided that the dielectric has no magnetic properties and losses are not considered. However, the electric field $\vec{E}$ inside the cavity is not known, and we must use some physical approximation for $\vec{E}$ in Eq. (3) to calculate the frequency shift.

To demonstrate the use of Eq. (3) and understand its physical meaning, consider the limit $\Delta\epsilon\rightarrow 0$ in which we can approximate ω, $\vec{E}$, and $\vec{H}$ by ω_0, $\vec{E}_0$, and $\vec{H}_0$, and obtain:

$$\frac{\omega-\omega_0}{\omega_0}=-\frac{\int_{V_d}\Delta\epsilon|E_0|^2\,dV}{2\int_{V_c}\epsilon|E_0|^2\,dV}. \tag{4}$$

From Eq. (4) we see that the introduction of a dielectric reduces the resonant frequencies. This fact is understood as follows. The presence of the dielectric decreases the wave velocity in the resonator. Because the wavelength is fixed by the cavity dimensions to meet the boundary conditions, the resonant frequency must decrease.

In the more general case where $\Delta\epsilon$ is not small, we cannot use the approximation $\vec{E}=\vec{E}_0$ in the numerator of Eq. (3). Instead, we assume that the electric field inside the dielectric, $\vec{E}_{\rm int}$, has the same form as $\vec{E}_0$ in Eq. (1), and that its amplitude $E^0_{\rm int}$ is related by the usual boundary conditions to the unperturbed electric field in the cavity. We have

$$\frac{\omega-\omega_0}{\omega}=-\frac{\int_{V_d}\Delta\epsilon\vec{E}_{\rm int}\vec{E}_0^*\,dV}{2\int_{V_c}\epsilon|E_0|^2\,dV}. \tag{5}$$

The frequency shift then depends on the dielectric shape and on its position inside the cavity.

We now discuss the characterization of the dielectric in our cavity. For clarity we restrict ourselves to the (110) mode. The frequency shift will be maximized if we place the dielectric at the center of the cavity, where the electric field has an absolute maximum. In this case we have

$$\frac{\omega-\omega_0}{\omega}=-\frac{\Delta\epsilon}{2\epsilon_0}\frac{E^0_{\rm int}}{E^0_z}\frac{l_z}{d}\times\left[\frac{l_x}{a}+\frac{1}{\pi}\sin\left(\frac{\pi l_x}{a}\right)\right]\left[\frac{l_y}{b}+\frac{1}{\pi}\sin\left(\frac{\pi l_y}{b}\right)\right], \tag{6}$$

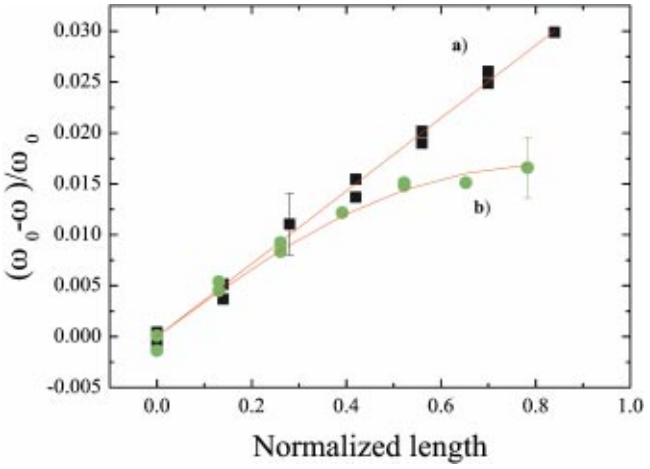

Fig. 4. The relative frequency variation as a function of dielectric dimensions. The two curves correspond to the geometries (b) and (c) in Fig. 1, which are designed to investigate the field characteristics. Curve (a) reflects the uniformity of the field along the z axis, and the saturation in curve (b) is due to the field decrease when going from the center to the sides along the y axis. [The relative length represents l_z/d and l_y/b in curves (a) and (b).]

where l_x, l_y, and l_z are the dimensions of the dielectric. We investigate two different geometries. In the first we pile several blocks ($177\times65\times35$ mm^3) containing a granulated dielectric [see Fig. 1(b)], which, given our wavelength, can be considered to be a continuum. The electric field $\vec{E}_0$ is directed along the z axis and is tangential to the main dielectric surface. The continuity of the tangential component of the electric field at a boundary suggests that we can substitute the internal field amplitude in the dielectric by E^0_z in Eq. (6), that is, $E^0_{\rm int}\approx E^0_z$. We show in Fig. 4 the dependence of the relative frequency variation on the dielectric height l_z/d, which is clearly linear as a result of the constant behavior of E^0_z with respect to z. A least squares fit to Eq. (6) yields $\epsilon_r=\epsilon/\epsilon_0=1.8\pm0.1$.

In the second geometry the blocks containing the dielectric are placed horizontally, side by side, maintaining the symmetric position of the blocks around the cavity center [see Fig. 1(c)]. The electric field is not uniform along the y direction and, in this geometry, the dependence of the frequency shift on l_y/b is no longer linear (see Fig. 4). If we again assume that $E^0_{\rm int}\approx E^0_z$, a least squares fit to Eq. (6) yields $\epsilon_r=1.7\pm0.1$, in agreement with our previous results.

Finally, we can compare the relative frequency variation in geometries (c) and (d) of Fig. 1, in which the dielectric in (c) is rotated by 90° with respect to the dielectric in (d). As we have seen, in geometry (c) the electric field is continuous across the dielectric boundary, and we take $E^0_{\rm int}\approx E^0_z$. With $l_y=390$ mm we obtain $(\omega_0-\omega)/\omega=0.017\pm0.003$. However, in geometry (d), the electric field is perpendicular to the main dielectric surface, and the electric displacement is continuous across the boundary. Therefore we have $\epsilon E^0_{\rm int}\approx\epsilon_0E^0_z$. The field inside the dielectric, as well as the frequency shift, are then reduced compared to those in geometry (c). With the same dielectric we have $(\omega_0-\omega)/\omega=0.010\pm0.003$. The ratio between the two shifts is the dielectric constant $\epsilon_r=1.7\pm0.5$, which again is in good agreement with previous results.

IV. SUMMARY

We have used a rectangular cavity to demonstrate the physics of cavity resonators. The rectangular geometry has several advantages. First, it avoids advanced mathematics and allows students to concentrate on the physics. It also is easy to modify the cavity dimensions and introduce different materials inside the cavity.

The stationary modes can be altered by changing the cavity length (see Fig. 3). Different modes can be suppressed by placing a metallic plate at the appropriate positions inside the cavity. Both modifications can be directly observed by students on an oscilloscope (Fig. 2).

The introduction of a dielectric introduces students to a dielectric characterization technique. Its use demonstrates the application of the appropriate boundary conditions. The frequency shift as a function of dielectric length (Fig. 4) reflects the electric field distribution in the cavity.

ACKNOWLEDGMENT

The authors thank S. Gilliland for a critical reading of the paper.

[a)]Electronic mail: julio.pellicer@uv.es

[1]Roald K. Wangsness, *Electromagnetic Fields* (Wiley, New York, 1979).

[2]Wolfgang K. H. Panofsky and Melba Phillips, *Classical Electricity and Magnetism* (Addison-Wesley, 1962).

[3]R. Feynman, R. B. Leighton, and M. Sands, *The Feynman Lectures on Physics* (Addison Wesley, New York, 1964), Vol. II.

[4]R. F. Harrington, *Time-Harmonic Electromagnetic Fields* (McGraw-Hill, New York, 1961).

ONLINE COLOR FIGURES AND AUXILIARY MATERIAL

AJP will now use author-provided color figures for its online version (figures will still be black and white in the print version). Figure captions and references to the figures in the text must be appropriate for both color and black and white versions. There is no extra cost for online color figures.

In addition AJP utilizes the Electronic Physics Auxiliary Publication Service (EPAPS) maintained by the American Institute of Physics (AIP). This low-cost electronic depository contains material supplemental to papers published through AIP. Appropriate materials include digital multimedia (such as audio, movie, computer animations, 3D figures), computer program listings, additional figures, and large tables of data.

More information on both these options can be found at www.kzoo.edu/ajp/.